

Attenuation of Cosmic Ray Electron Boosted Dark Matter

Tim Herbermann^{✉,*}, Manfred Lindner[†] and Manibrata Sen^{✉‡}

Max-Planck-Institut für Kernphysik, Saupfercheckweg 1, 69117 Heidelberg, Germany

(Dated: August 7, 2024)

We consider a model of boosted dark matter (DM), where a fraction of DM is upscattered to relativistic energies by cosmic ray electrons. Such interactions responsible for boosting the DM also attenuate its flux at the Earth. Considering a simple model of constant interaction cross-section, we make analytical estimates of the variation of the attenuation ceiling with the DM mass and confirm it numerically. We then extend our analysis to a Z' -mediated leptophilic DM model. We show that the attenuation ceiling remains nearly model-independent for DM and mediator particles heavier than the electron, challenging some previous discussions on this topic. Using the XENONnT direct detection experiment, we illustrate how constraints based on energy-dependent scattering can significantly differ from those based on an assumed constant cross-section. This highlights the importance of re-evaluating these constraints in the context of specific models.

Introduction – Despite the remarkable success of the Standard Model (SM) of particle physics, it only ends up explaining about $\sim 15\%$ of the total matter content of the Universe. The remaining 85%, accounted for by the elusive Dark Matter (DM), is an indispensable part of our Universe and is invoked to explain various unaccounted-for observations, like the rotation curves of galaxies, lensing of galaxy clusters as well as anisotropies of the cosmic microwave background (CMB). However, when it comes to the nature of DM, we are still in the dark – decades of ongoing searches have not yet shed any light [1, 2].

One of the key strategies in the search for DM is through direct detection, in which a search of energy depositions of ambient DM from the Galactic halo upon interaction with nucleons in the detector is explored [3]. Although there has not been a detection so far, recent experiments like XENON [4], LUX-Zepelin (LZ) [5, 6] and PandaX [7] continue to push the detection limits. The detection prospects for these nuclear recoil searches are severely limited by the kinematics of energy deposition for sub-GeV low-mass DM [8]. To gain sensitivity to lower mass regimes, electron-DM scattering has been adopted as an additional detection channel and is being searched to probe low-mass DM [9–12].

A lucrative idea to overcome the low DM mass suppression in current experiments is to search for signals from boosted dark matter (BDM). The idea is simple – if by some mechanism, a subdominant fraction of DM is boosted to (semi-)relativistic energies, the kinematic suppression of the detection signal can be avoided. The proposal to consider upscattering by hadronic cosmic rays (CR) has been extensively studied in the literature [13–28]. Additionally, new mechanisms for boosting the DM candidate have been explored, which involve upscattering by neutrinos, inelastic DM, decays of heavier components of a multi-component dark sector, and so on [29–43].

Searches for upscattered DM have the distinct advantage of not requiring additional assumptions about new interactions between the SM and DM. The interactions considered for direct detection naturally result in the formation of a population of BDM through scattering with CR electrons and nucleons. Consequently, a subdominant composition of BDM is inevitably present. However, detecting this boosted component of DM is challenging because the additional powers of the interaction coupling necessary for the boosting process also end up suppressing it. Furthermore, the BDM spectrum is also attenuated due to interaction with nucleons and electrons in the Earth.

To derive constraints on DM-nucleon/electron scattering cross-sections arising out of CR-BDM, some of the earlier works focused on a constant energy-independent cross-section model [13–15, 25]. This assumption of an effective cross-section need not hold for the entire energy range of scattering, thereby necessitating the requirement of a *model-dependent* treatment [24, 27]. Furthermore, the attenuation treatment in these studies is usually very complicated and requires a numerical solution for a detailed analysis. In fact, for a realistic estimate with multiple scatterings, one needs to use Monte-Carlo simulations [34, 44] (however, see [44] for an analytical comparison). In [26], a semi-analytical prescription was presented without resorting to a full Monte-Carlo treatment of the attenuation effect. The constraints derived predicted the presence of an attenuation ceiling dependent on the mass of the mediator, even for large DM masses. Moreover, for energy-independent scattering, the attenuation ceiling, derived from [24] is shown to be a constant and independent of the DM and the mediator masses.

In this *Letter*, we reconsider the scenario of upscattering of DM by CR electrons by revisiting the treatment of attenuation of BDM. Under the assumption of a constant interaction cross-section, we first perform analytical estimates of the effect of attenuation on BDM, which we confirm numerically. We demonstrate analytically the presence of an almost *model-independent* attenuation ceiling for large DM masses, in contrast to the findings presented in some previous studies. We further generalise

* tim.herbermann@mpi-hd.mpg.de

† lindner@mpi-hd.mpg.de

‡ manibrata.sen@mpi-hd.mpg.de

our results to include energy-dependent scattering for a Z' mediated leptophilic DM model and confirm that the attenuation ceiling depends only mildly on the mediator mass. We perform a detailed study of how XENONnT can constrain such models of BDM and demonstrate that constraints for an energy-dependent scattering can differ considerably from those derived under the assumptions of a constant cross-section.

Cosmic ray electron upscattered dark matter – Energetic CR electrons scattering off the ambient DM can boost the latter to kinetic energies significantly exceeding that from virial motion. The kinetic energy of the DM of mass m_χ is given by

$$T_\chi = T_\chi^{\max} \left(\frac{1 - \cos \theta}{2} \right), \quad (1)$$

$$T_\chi^{\max} = \frac{T_e^2 + 2m_e T_e}{T_e + (m_\chi + m_e)^2 / 2m_\chi}.$$

Here θ is the scattering angle in the centre of momentum frame, while T_e and m_e denote the CR electron kinetic energy in the laboratory frame and its mass respectively. The maximum energy that DM can gain in the laboratory frame is T_χ^{\max} .

The upscattered DM flux is given by the local upscattering rate from CR electrons, weighted by the ambient DM density and reads

$$\frac{d\Phi_\chi}{dT_\chi} = D_{\text{eff}} \rho_{\chi, \text{loc}} \int_{T_e^{\min}}^{\infty} dT_e \frac{1}{m_\chi} \frac{d\Phi_e}{dT_e} \frac{d\sigma_{e\chi}}{dT_\chi}. \quad (2)$$

Here $\rho_{\chi, \text{loc}}$ is the local energy density of DM, which we fix to 0.4 GeV cm^{-3} and D_{eff} is the effective distance to which we include CR electron boosted DM. We use $D_{\text{eff}} = 1 \text{ kpc}$, only including contributions from our galactic neighborhood. This is conservative since the CR electron flux is only known locally and is subject to considerable astrophysical uncertainties. The minimum electron energy T_e^{\min} to accelerate DM to a kinetic energy of T_χ follows directly from kinematic considerations and can be calculated from inverting the expression for T_χ^{\max} in Eq. 1.

To perform our computations, we use an analytic parameterisation of the local CR electron spectrum from [45]. The spectra is presented from 2 MeV to 90 GeV and we extrapolate to lower energies, if necessary. The CR electron spectrum, shown in Fig. 1, demonstrates the well-known power-law feature.

Eq. 2 can be solved numerically under the assumption of an effective constant cross-section, such that $d\sigma_{e\chi}/dT_\chi = \bar{\sigma}_{e\chi}/T_\chi^{\max}$. As a demonstration, an example BDM spectrum is shown in blue dashed lines in Fig. 1 for a benchmark point $m_\chi = 10 \text{ MeV}$ and $\bar{\sigma}_{e\chi} = 10^{-29} \text{ cm}^2$. This demonstrates that the BDM spectra, in absence of attenuation, can have a shape similar to that of the CR electrons, albeit with a very different normalisation. We expect this to change when attenuation is included, which we will describe next.

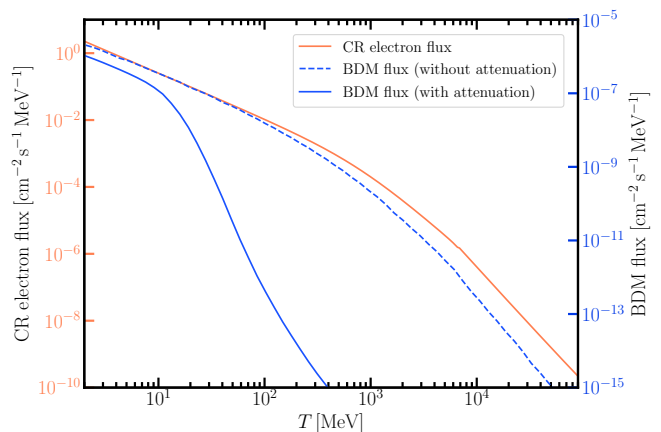


FIG. 1. The CR electron flux (in red) used to boost DM and the resulting spectrum of BDM flux (in blue). For the BDM computation, we assume a constant cross-section for a benchmark point $m_\chi = 10 \text{ MeV}$ and $\bar{\sigma}_{e\chi} = 10^{-29} \text{ cm}^2$. We show the BDM flux with (blue, solid) and without (blue, dashed) attenuation of DM flux in the Earth to highlight the importance of attenuation. Note the two different value ranges for the respective axes.

Attenuation in the Earth – To model the energy loss of DM traversing a medium we adopt the widely used mean energy loss equation [13, 14, 16, 43]

$$\frac{dT_\chi}{dx}(x) = -n_e \int_0^{T_e^{\max}} dT_e T_e \frac{d\sigma_{e\chi}}{dT_e}, \quad (3)$$

where T_e^{\max} is the maximum energy of recoil, evaluated in a manner similar to Eq. 1. We fix the electron density in the Earth to $n_e = 8 \times 10^{23} \text{ cm}^{-3}$ [41]. For $T_\chi \ll m_e$ and assuming $d\sigma_{e\chi}/dT_e = \bar{\sigma}_{e\chi}/T_e^{\max}$, Eq. 3 can be solved analytically to estimate the effect of attenuation. The solid blue line in Fig. 1 shows the BDM spectrum after attenuation for a detector at depth $d = 1.4 \text{ km}$. It is evident how the inclusion of attenuation significantly alters the BDM flux at the detector site. We observe an overall reduction of flux for all energies, but it is particularly pronounced for large kinetic energies where a complete loss of BDM flux is present.

However, if the target particles are electrons, the validity of the above approximation is not guaranteed and the hierarchy of energy scales in the problem is more subtle. To shed light on this issue, we consider the full energy dependence of cross-sections for specific models and resort to a numerical solution. We adopt a framework similar to the study on DSNB-boosted DM by two of the authors, which solved Eq. 3 numerically without any assumed hierarchy of energy scales [43]. We also consider the absence of multiple scattering with electrons, and hence our estimate is still conservative.

While a simple analytical solution breaks down in some cases, we can still consider it to gain some intuition on the general behaviour of the numerical solution in different regimes. To this end, we solve Eq. 3 for an energy

independent cross-section $\bar{\sigma}_{e\chi}$ and find

$$\frac{dT_\chi}{dx} = -\frac{1}{2}n_e\bar{\sigma}_{e\chi}\frac{T_\chi^2 + 2m_\chi T_\chi}{T_\chi + \frac{(m_e+m_\chi)^2}{2m_e}}. \quad (4)$$

To study the behaviour of the mean energy loss, we consider the heavy DM regime ($m_\chi \gg m_e$), the intermediate regime ($m_\chi \sim m_e$), and the light DM regime ($m_\chi \ll m_e$).

a. Heavy DM regime. We consider the heavy DM limit, i.e. $m_\chi \gg m_e, T_\chi$, where the inequality with respect to T_χ is understood to be valid for the bulk of boosted DM flux that gives a direct detection signal and not necessarily for the entire BDM spectrum. In this case, mimicking the approximation previously made for energy loss due to scattering on nucleons (e.g.[13]), we find

$$\frac{dT_\chi}{dx} = -\frac{1}{2m_\chi\lambda_{\text{eff}}}(T_\chi^2 + 2m_\chi T_\chi), \quad (5)$$

with the effective length scale of energy loss $\lambda_{\text{eff}}^{-1} = 4n_e\bar{\sigma}_{e\chi}m_e m_\chi / (m_e + m_\chi)^2$. A suitable criterion for attenuation is $d/\lambda_{\text{eff}} \approx 1$ for a detector at depth d . This leads to a solution where effective cross-section for attenuation scales as $\bar{\sigma}_{e\chi} \propto m_\chi$.

b. Intermediate regime. The location of the attenuation ceiling can be estimated in the regime $m_\chi \sim m_e$. Setting $m_\chi \sim m_e \sim m$ simplifies the energy loss equation to

$$\frac{dT_\chi}{dx} = -\frac{1}{2}n_e\bar{\sigma}_{e\chi}T_\chi\left(\frac{T_\chi + 2m}{T_\chi + 2m}\right) \approx -\frac{1}{2}n_e\bar{\sigma}_{e\chi}T_\chi. \quad (6)$$

This gives rise to an exponential suppression with a characteristic scale $\lambda_{\text{eff}}^{-1} = n_e\bar{\sigma}_{e\chi}/2$. Using the same argument as before for a detector at depth d , we find a constant attenuation ceiling at $\bar{\sigma}_{e\chi} = 2/(n_e d)$.

c. Light DM regime. Going to even lower DM masses, $m_\chi \ll m_e$, we infer from T_χ^{max} in Eq.1 that T_χ scales as $T_\chi \sim 2m_\chi T_{e,\text{CR}}^2 / (2m_\chi T_{e,\text{CR}} + m_e^2)$, where $T_{e,\text{CR}}^2 \gg m_e$ is the CR electron kinetic energy. Since CR electrons are relativistic, $T_\chi \gg m_\chi$ holds for most of the energy range. Thus the energy loss equation approximates to

$$\frac{dT_\chi}{dx} = -\frac{n_e\bar{\sigma}_{e\chi}}{2}\frac{T_\chi^2}{T_\chi + \frac{m_e}{2}}. \quad (7)$$

An analytic solution can be written in terms of the Lambert-W function as a function of $\lambda_{\text{eff}}^{-1} = n_e\bar{\sigma}_{e\chi}$. We note that the precise scaling of energy loss is non-trivial and depends on the constant of integration, i.e., on the initial kinetic energy of the BDM particle. So while we cannot reliably predict the precise value, we may still infer that the location should be largely independent of m_χ . Hence, we expect again a constant attenuation ceiling, albeit at different numerical values of $\bar{\sigma}_{e\chi}$ due to the potentially much weaker suppression. These analytical estimates allow us to understand the dynamics of

attenuation of BDM due to the scattering by electrons in the atmosphere and the earth. As seen from Fig. 2, the analytical estimates give an excellent prediction of the behaviour of the attenuation ceiling obtained by solving Eq. 3 numerically.

Although these estimates are performed for a constant cross-section, we expect the conclusion to qualitatively hold for fully energy-dependent cross-sections as well. To understand this, we can decompose the integral in Eq 3 as $\frac{1}{2}T_e^{\text{max}}\bar{\sigma}_{e\chi} \times f(T_\chi)$, where $\frac{d\bar{\sigma}_{e\chi}}{dT_e} = \frac{\bar{\sigma}_{e\chi}}{T_e^{\text{max}}}$ and $f(T_\chi)$ is an effective form factor that encodes deviations from the constant cross-section assumption. Note that both the effective cross-section as well as the effective form factor have an explicit model dependence. Hence, the attenuation is well described by a constant cross-section, $\bar{\sigma}_{e\chi}$, modulated by a model-dependence coming from $f(T_\chi)$. We find that as long as $f(T_\chi) \sim 1$, the general properties, including the position of the attenuation ceiling, are reproduced and independent of the details of the underlying interaction.

Event rates and statistical analysis – The non-observation of BDM event rates in direct detection experiments can be used to constrain DM-electron scatterings. In this work, we restrict our analysis to electron recoil searches by the XENON collaboration [9]. We expect from our previous studies of supernova neutrino background-BDM that the constraints arising from other direct detection experiments like LZ [5] and PandaX [7] will be qualitatively similar, although some differences may arise due to the different overburden.

The predicted event rate is calculated as

$$\frac{dR}{dT_e} = N_e \int dT_\chi \frac{d\Phi_\chi}{dT_\chi^x} \frac{d\sigma_{e\chi}}{dT_e}, \quad (8)$$

where T_χ^x is the solution of Eq.3, giving the DM kinetic energy loss as a function of depth, and $N_e = Z_{\text{eff}}(T_e)M_{\text{det}}/m_{\text{Xe}}$ denotes the number of electron targets in the detector. Typically, the effective charge number $Z_{\text{eff}}(T_e)$ is energy-dependent, though we assume constant $Z_{\text{eff}}(T_e) \approx 40$. To calculate the flux of BDM $d\Phi_\chi/dT_\chi^x$, a detector depth of $h_d = 1.4\text{km}$ is assumed. We take the convolution of the rate with a Gaussian resolution function centred around the reconstructed energy E_R and use a resolution of $\sigma_{\text{XE}} = 0.31\sqrt{E/\text{keV}} + 0.0037E/\text{keV}$ [46]. The convoluted signal is multiplied by the respective efficiency function.

To derive constraints on the DM mass and the couplings of the model, we employ the following χ^2 statistic,

$$\chi^2 = \sum_{E_i} \frac{(R_i^{\text{pred}} - R_i^{\text{exp}})^2}{\sigma_i^2}. \quad (9)$$

Here R_i^{pred} is the predicted event rate from the best-fit background model and the additional CR boosted DM contribution. Measured event rates are indicated as R_i^{exp} . We use published experimental uncertainties (σ_{Di}) and

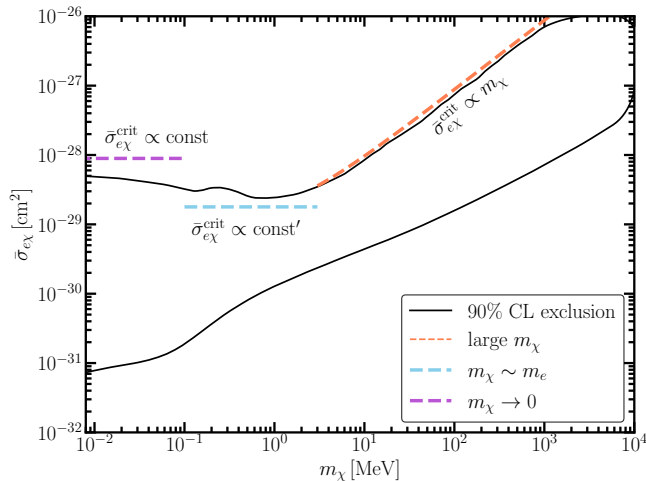


FIG. 2. Numerically determined exclusion contour and attenuation ceiling for constant cross-section scenario compared to the approximate analytical solutions in the small, intermediate and large m_χ limit, in the $m_\chi - \bar{\sigma}_{e\chi}$ plane. For heavy m_χ , we note a good agreement with the numerical result, whereas for lighter results we cannot predict the precise value but are limited to qualitative statements on the scaling with m_χ .

combine those with a Poissonian counting error on the total predicted event rate, i.e. $\sigma_i^2 = R_i^{\text{pred}} + \sigma_{\text{Di}}^2$. To exclude regions of parameter space, we use a χ^2 difference to the best-fit background model, i.e. $\Delta\chi^2 = \chi^2 - \chi_{\text{bkg}}^2$ and use $\Delta\chi^2 > 4.61$ to reject at 90% confidence level (CL). Any constraints put from this statistical model are conservative, as in they do not attempt a joint fit of background and signal which would require a more involved statistical model.

We first demonstrate our constraints for the case of the constant effective cross-section, i.e., $d\sigma_{e\chi}/dT_{\chi,e} = \bar{\sigma}_{e\chi}/T_{\chi,e}^{\text{max}}$, in a XENON-like setup in Fig. 2. We compare the numerically determined exclusion contour with the analytic estimates for the attenuation ceiling. The limit $m_\chi \gg m_e$ is captured perfectly by the analytical approximation - the numerical solution exhibits approximately the same exponential energy loss that determines the attenuation limit. In the regime $m_\chi \sim m_e$, the approximations ensure a qualitative agreement, predicting the turnover of the attenuation ceiling. This also demonstrates that the position of the attenuation ceiling is largely independent of m_χ in this regime. The limit $m_\chi \ll m_e$, however, is less well determined. The reason is two-fold: There is an explicit dependence on the initial energy of the particle and energy loss from attenuation is no longer exponential but rather follows a complicated functional dependence that is much weaker. However, we can still predict qualitatively a ceiling that is, within the scope of the approximations made, largely independent of m_χ , a behaviour that we also find in the full numerical solution which exhibits a very weak dependence on m_χ . This is in contrast to some previous studies [24], which

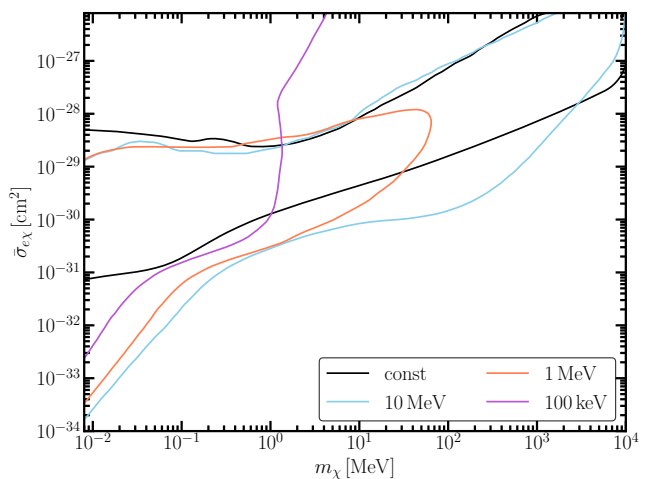


FIG. 3. Constraints cast on the parameter space for our Z' -model. The coloured shaded regions show limits at 90% CL for different masses of the mediator and present results in terms of DM mass and the effective cross-section $m_\chi - \bar{\sigma}_{e\chi}$ plane. To allow comparison to previous results. The constraint from a constant cross-section calculation is shown in black.

find little to no significant dependence of the attenuation ceiling on the DM mass even in the case of constant cross-section.

We now turn to demonstrate the model-dependence of the results, through a model of DM-electron interaction through a massive vector gauge boson. The SM can be extended with a singlet Dirac DM χ coupled to a massive vector boson Z'_μ . This can be embedded in the SM with an additional gauge U(1) symmetry, like $L_e - L_\mu$, $L_e - L_\tau$ or a flavour universal one [47]. We remain agnostic of the details of the complete model. The relevant interactions for boosting and detecting the DM are

$$\mathcal{L} \supset g_e \bar{e} \gamma^\mu e Z'_\mu + g_\chi \bar{\chi} \gamma^\mu \chi Z'_\mu. \quad (10)$$

Note that in this case, the effective cross-section becomes model-dependent and is defined through,

$$\bar{\sigma}_{e\chi} = \frac{g^4}{\pi} \frac{\mu_{e\chi}^2}{(q_{\text{ref}}^2 + m_{Z'}^2)^2}, \quad (11)$$

where $\mu_{e\chi}$ is the reduced mass of the electron-DM-system and $g = \sqrt{g_e g_\chi}$ is an effective coupling. The conventional definition of $q_{\text{ref}} = \alpha m_e$ involves the fine-structure constant. Using this parameterisation allows for easy comparison to previous studies.

Fig. 3 shows the constraints on the $m_\chi - \bar{\sigma}_{e\chi}$ plane for different Z' masses. To compare our results, we show the constraints on the constant cross-section model in black. As discussed before, the constraints are strongly dependent on the mediator mass and can change drastically for a low-mass mediator. Even when the mediator is heavy, the constraint can be quite different from the constant cross-section case, especially for low DM masses. In light

of our discussion on the approximate solutions, we can attempt to understand the general behaviour of the exclusion contours and especially the attenuation ceiling.

In the limit of large m_χ and $m_{Z'}$, the attenuation ceiling is universal and model-independent. In this limit, the integral part of the energy loss equation (Eq. 3) is well approximated by the same integral assuming the effective cross-section (Eq. 11) the model is mapped on. Since the energy loss is an integrated effect, we are less sensitive to explicit energy dependence. Towards smaller m_χ the attenuation part of the contour becomes increasingly more model-dependent and moderate differences between mediator masses are observable. This is largely driven by the effective $\bar{\sigma}_{e\chi}$ becoming a poorer approximation to the actual cross-section. For very small DM masses, the attenuation ceiling falls off strongly with decreasing mass. This effect is an artefact of the definition of $\bar{\sigma}_{e\chi}$. Indeed, as $m_\chi \rightarrow 0$ we find $\bar{\sigma}_{e\chi} \propto m_\chi^2$.

For light mediators, $m_{Z'} < m_e$, the obtained contours are significantly different. This is primarily because the light mediator regime is qualitatively very different from the heavy mediator and constant cross-section cases in terms of the differential cross-section, as mediator masses start becoming relevant. Moreover, the commonly adapted $\bar{\sigma}_{e\chi}$ parameterisation is also a very poor proxy for the actual cross-section in light mediator models of BDM. This highlights once more the necessity of model-dependent studies in the direct detection of BDM, in tandem with what was presented in [27].

Conclusion – Boosted Dark Matter (BDM) offers a way to derive complementary constraints on Dark Matter (DM) models. When a model assumes certain interactions that permit direct detection searches, an irreducible background of BDM is almost inevitable, provided there is a suitable upscattering mechanism. In this study, we examined the upscattering of light leptophilic DM by cosmic ray electrons. By focusing on a minimal DM model where interactions are mediated by a massive vector mediator, we obtained updated constraints on DM-electron interactions using data from XENONnT, covering the mass range from 10 keV to 10 GeV. We emphasise the strong model dependence of experimental signatures and constraints in BDM studies, particularly exploring the attenuation of the BDM flux in the medium before it

reaches underground detectors.

Regarding the attenuation of BDM in the Earth, we made the conservative assumption of a single scattering between BDM and electrons in the Earth. Firstly, under the assumption of a constant interaction cross-section, we provide analytic expressions for the effect of attenuation on the BDM flux. We further confirmed through a detailed numerical solution the excellent agreement of our analytic approximations with the full solution.

We used our understanding of the constant cross-section analysis to generalise to the case with energy-dependent interaction cross-sections. Under the assumption of vector-mediated interaction between DM and electron, we demonstrated how the constraints imposed from a direct detection experiment like XENONnT can be very different for energy-dependent scattering as opposed to the constraints derived from an effective constant cross-section interaction. Compared to similar previous studies [24, 26], we note significant qualitative and quantitative deviations, especially when including the effect of attenuation. In particular, we showed the presence of a model-independent attenuation ceiling in the presence of large DM and mediator masses. These previous studies adopted different approximation schemes, for example, considerations of critical energy loss [24] or including multiple scatterings [26]. In our study, even though we omit multiple scattering and the possibility of back-scattering into the atmosphere, the effect of attenuation is stronger. Since our assumptions are conservative and minimal, we expect our results for energy loss of BDM to be robust.

In light of the absence of an unequivocal direct detection of dark matter, our work highlights the importance of addressing new approaches to its direct detection. Boosted dark matter sourced from upscattering by energetic particles, promises to be a powerful tool to probe dark matter light dark matter in current experiments.

Acknowledgments – We thank Paul Frederik Depta for helpful comments on the numerical approach. TH acknowledges support by the IMPRS-PTFS. MS thanks the Galileo Galilei Institute for Theoretical Physics for the hospitality and the INFN for partial support during the completion of this work.

-
- [1] G. Bertone and D. Hooper, History of dark matter, *Rev. Mod. Phys.* **90**, 045002 (2018), arXiv:1605.04909 [astro-ph.CO].
 - [2] N. Aghanim *et al.* (Planck), Planck 2018 results. VI. Cosmological parameters, *Astron. Astrophys.* **641**, A6 (2020), [Erratum: *Astron. Astrophys.* 652, C4 (2021)], arXiv:1807.06209 [astro-ph.CO].
 - [3] M. Schumann, Direct Detection of WIMP Dark Matter: Concepts and Status, *J. Phys. G* **46**, 103003 (2019), arXiv:1903.03026 [astro-ph.CO].
 - [4] E. Aprile *et al.* (XENON), First Dark Matter Search with Nuclear Recoils from the XENONnT Experiment, *Phys. Rev. Lett.* **131**, 041003 (2023), arXiv:2303.14729 [hep-ex].
 - [5] J. Aalbers *et al.* (LZ), First Dark Matter Search Results from the LUX-ZEPLIN (LZ) Experiment, *Phys. Rev. Lett.* **131**, 041002 (2023), arXiv:2207.03764 [hep-ex].
 - [6] J. Aalbers *et al.* (LZ), Background determination for the LUX-ZEPLIN dark matter experiment, *Phys. Rev. D* **108**, 012010 (2023), arXiv:2211.17120 [hep-ex].
 - [7] D. Zhang *et al.* (PandaX), Search for Light Fermionic Dark Matter Absorption on Electrons in PandaX-4T,

- Phys. Rev. Lett. **129**, 161804 (2022), arXiv:2206.02339 [hep-ex].
- [8] R. Essig *et al.*, Snowmass2021 Cosmic Frontier: The landscape of low-threshold dark matter direct detection in the next decade, in *Snowmass 2021* (2022) arXiv:2203.08297 [hep-ph].
- [9] E. Aprile *et al.* (XENON), Search for New Physics in Electronic Recoil Data from XENONnT, Phys. Rev. Lett. **129**, 161805 (2022), arXiv:2207.11330 [hep-ex].
- [10] I. Arnquist *et al.* (DAMIC-M), First Constraints from DAMIC-M on Sub-GeV Dark-Matter Particles Interacting with Electrons, Phys. Rev. Lett. **130**, 171003 (2023), arXiv:2302.02372 [hep-ex].
- [11] P. Adari *et al.* (SENSEI), SENSEI: First Direct-Detection Results on sub-GeV Dark Matter from SENSEI at SNOLAB, (2023), arXiv:2312.13342 [astro-ph.CO].
- [12] D. W. Amaral *et al.* (SuperCDMS), Constraints on low-mass, relic dark matter candidates from a surface-operated SuperCDMS single-charge sensitive detector, Phys. Rev. D **102**, 091101 (2020), arXiv:2005.14067 [hep-ex].
- [13] T. Bringmann and M. Pospelov, Novel direct detection constraints on light dark matter, Phys. Rev. Lett. **122**, 171801 (2019), arXiv:1810.10543 [hep-ph].
- [14] Y. Ema, F. Sala, and R. Sato, Light Dark Matter at Neutrino Experiments, Phys. Rev. Lett. **122**, 181802 (2019), arXiv:1811.00520 [hep-ph].
- [15] C. V. Cappiello, K. C. Y. Ng, and J. F. Beacom, Reverse Direct Detection: Cosmic Ray Scattering With Light Dark Matter, Phys. Rev. D **99**, 063004 (2019), arXiv:1810.07705 [hep-ph].
- [16] J. B. Dent, B. Dutta, J. L. Newstead, and I. M. Shoemaker, Bounds on Cosmic Ray-Boosted Dark Matter in Simplified Models and its Corresponding Neutrino-Floor, Phys. Rev. D **101**, 116007 (2020), arXiv:1907.03782 [hep-ph].
- [17] W. Wang, L. Wu, J. M. Yang, H. Zhou, and B. Zhu, Cosmic ray boosted sub-GeV gravitationally interacting dark matter in direct detection, JHEP **12**, 072, [Erratum: JHEP **02**, 052 (2021)], arXiv:1912.09904 [hep-ph].
- [18] J. Alvey, M. Campos, M. Fairbairn, and T. You, Detecting Light Dark Matter via Inelastic Cosmic Ray Collisions, Phys. Rev. Lett. **123**, 261802 (2019), arXiv:1905.05776 [hep-ph].
- [19] G. Guo, Y.-L. S. Tsai, M.-R. Wu, and Q. Yuan, Elastic and Inelastic Scattering of Cosmic-Rays on Sub-GeV Dark Matter, Phys. Rev. D **102**, 103004 (2020), arXiv:2008.12137 [astro-ph.HE].
- [20] G. Guo, Y.-L. S. Tsai, M.-R. Wu, and Q. Yuan, Elastic and inelastic scattering of cosmic rays on sub-gev dark matter, Physical Review D **102**, 10.1103/physrevd.102.103004 (2020).
- [21] J. B. Dent, B. Dutta, J. L. Newstead, I. M. Shoemaker, and N. T. Arellano, Present and future status of light dark matter models from cosmic-ray electron upscattering, Phys. Rev. D **103**, 095015 (2021), arXiv:2010.09749 [hep-ph].
- [22] C. Xia, Y.-H. Xu, and Y.-F. Zhou, Production and attenuation of cosmic-ray boosted dark matter, JCAP **02** (02), 028, arXiv:2111.05559 [hep-ph].
- [23] N. F. Bell, J. B. Dent, B. Dutta, S. Ghosh, J. Kumar, J. L. Newstead, and I. M. Shoemaker, Cosmic-ray upscattered inelastic dark matter, Phys. Rev. D **104**, 076020 (2021), arXiv:2108.00583 [hep-ph].
- [24] D. Bardhan, S. Bhowmick, D. Ghosh, A. Guha, and D. Sachdeva, Bounds on boosted dark matter from direct detection: The role of energy-dependent cross sections, Phys. Rev. D **107**, 015010 (2023), arXiv:2208.09405 [hep-ph].
- [25] T. N. Maity and R. Laha, Cosmic-ray boosted dark matter in Xe-based direct detection experiments, Eur. Phys. J. C **84**, 117 (2024), arXiv:2210.01815 [hep-ph].
- [26] A. Guha and J.-C. Park, Constraints on cosmic-ray boosted dark matter with realistic cross section, (2024), arXiv:2401.07750 [hep-ph].
- [27] N. F. Bell, J. L. Newstead, and I. Shaukat-Ali, Cosmic-ray boosted dark matter confronted by constraints on new light mediators, Phys. Rev. D **109**, 063034 (2024), arXiv:2309.11003 [hep-ph].
- [28] C. Cappiello, Q. Liu, G. Mohlabeng, and A. C. Vincent, Cosmic Ray-Boosted Dark Matter at IceCube, (2024), arXiv:2405.00086 [hep-ph].
- [29] K. Agashe, Y. Cui, L. Necib, and J. Thaler, (In)direct Detection of Boosted Dark Matter, JCAP **10**, 062, arXiv:1405.7370 [hep-ph].
- [30] J. Berger, Y. Cui, and Y. Zhao, Detecting Boosted Dark Matter from the Sun with Large Volume Neutrino Detectors, JCAP **02**, 005, arXiv:1410.2246 [hep-ph].
- [31] H. An, M. Pospelov, J. Pradler, and A. Ritz, Directly Detecting MeV-scale Dark Matter via Solar Reflection, Phys. Rev. Lett. **120**, 141801 (2018), [Erratum: Phys.Rev.Lett. **121**, 259903 (2018)], arXiv:1708.03642 [hep-ph].
- [32] W. Yin, Highly-boosted dark matter and cutoff for cosmic-ray neutrinos through neutrino portal, EPJ Web Conf. **208**, 04003 (2019), arXiv:1809.08610 [hep-ph].
- [33] W. DeRocco, P. W. Graham, D. Kasen, G. Marques-Tavares, and S. Rajendran, Supernova signals of light dark matter, Phys. Rev. D **100**, 075018 (2019), arXiv:1905.09284 [hep-ph].
- [34] T. Emken and C. Kouvaris, How blind are underground and surface detectors to strongly interacting Dark Matter?, Phys. Rev. D **97**, 115047 (2018), arXiv:1802.04764 [hep-ph].
- [35] Y. Chen, M.-Y. Cui, J. Shu, X. Xue, G.-W. Yuan, and Q. Yuan, Sun heated MeV-scale dark matter and the XENON1T electron recoil excess, JHEP **04**, 282, arXiv:2006.12447 [hep-ph].
- [36] H. An, H. Nie, M. Pospelov, J. Pradler, and A. Ritz, Solar reflection of dark matter, Phys. Rev. D **104**, 103026 (2021), arXiv:2108.10332 [hep-ph].
- [37] A. Das and M. Sen, Boosted dark matter from diffuse supernova neutrinos, Phys. Rev. D **104**, 075029 (2021), arXiv:2104.00027 [hep-ph].
- [38] Y. Jho, J.-C. Park, S. C. Park, and P.-Y. Tseng, Cosmic-Neutrino-Boosted Dark Matter (ν BDM), (2021), arXiv:2101.11262 [hep-ph].
- [39] A. Granelli, P. Ullio, and J.-W. Wang, Blazar-boosted dark matter at Super-Kamiokande, JCAP **07** (07), 013, arXiv:2202.07598 [astro-ph.HE].
- [40] T. Emken, Solar reflection of light dark matter with heavy mediators, Phys. Rev. D **105**, 063020 (2022), arXiv:2102.12483 [hep-ph].
- [41] V. De Romeri, A. Majumdar, D. K. Papoulias, and R. Srivastava, XENONnT and LUX-ZEPLIN constraints on DSNB-boosted dark matter, JCAP **03**, 028, arXiv:2309.04117 [hep-ph].

- [42] C. Xia, C.-Y. Xing, and Y.-H. Xu, Boosted Dark Matter From Centaurus A and Its Detection 10.1007/JHEP03(2024)076 (2024), arXiv:2401.03772 [hep-ph].
- [43] A. Das, T. Herbermann, M. Sen, and V. Takhistov, Energy-dependent boosted dark matter from diffuse supernova neutrino background, JCAP **07**, 045, arXiv:2403.15367 [hep-ph].
- [44] C. V. Cappiello, Analytic Approach to Light Dark Matter Propagation, Phys. Rev. Lett. **130**, 221001 (2023), arXiv:2301.07728 [hep-ph].
- [45] M. J. Boschini *et al.*, HelMod in the works: from direct observations to the local interstellar spectrum of cosmic-ray electrons, Astrophys. J. **854**, 94 (2018), arXiv:1801.04059 [astro-ph.HE].
- [46] E. Aprile, J. Aalbers, F. Agostini, M. Alfonsi, L. Althueser, F. Amaro, V. Antochi, E. Angelino, J. Angevaere, F. Arneodo, and et al., Excess electronic recoil events in xenon1t, Physical Review D **102**, 10.1103/physrevd.102.072004 (2020).
- [47] M. Bauer, P. Foldenauer, and J. Jaeckel, Hunting All the Hidden Photons, JHEP **07**, 094, arXiv:1803.05466 [hep-ph].